

# Transient Weak-Lensing by Cosmological Dark Matter Microhaloes

Sohrab Rahvar,<sup>1,2,\*</sup> Shant Baghram,<sup>3,1,4,†</sup> and Niayesh Afshordi<sup>3,1,‡</sup>

<sup>1</sup>*Perimeter Institute for Theoretical Physics, 31 Caroline St. N., Waterloo, ON, N2L 2Y5, Canada*

<sup>2</sup>*Department of Physics, Sharif University of Technology, P.O.Box 11365-9161, Tehran, Iran*

<sup>3</sup>*Department of Physics and Astronomy, University of Waterloo,*

*200 University Avenue West, Waterloo, ON, N2L 3G1, Canada*

<sup>4</sup>*School of Astronomy, Institute for Research in Fundamental Sciences (IPM), P. O. Box 19395-5531, Tehran, Iran*

We study the time variation of the apparent flux of cosmological point sources due to the transient weak lensing by dark matter microhaloes. Assuming a transverse motion of microhaloes with respect to our line of sight, we derive the correspondence between the temporal power spectrum of the weak lensing magnification, and the spatial power spectrum of density on small scales. Considering different approximations for the small scale structure of dark matter, we predict the apparent magnitude of cosmological point sources to vary by as much as  $10^{-4} - 10^{-3}$ , due to this effect, within a period of a few months. This red photometric noise has an almost perfect gaussian statistics, to one part in  $\sim 10^4$ . We also compare the transient weak lensing power spectrum with the background effects such as the stellar microlensing on cosmological scales. A quasar lensed by a galaxy or cluster like SDSSJ1004+4112 strong lensing system, with multiple images, is a suitable system for this study as: (i) using the time-delay method between different images, we can remove the intrinsic variations of the quasar, and (ii) strong lensing enhances signals from the transient weak lensing. We also require the images to form at large angular separations from the center of the lensing structure, in order to minimize contamination by the stellar microlensing. With long-term monitoring of quasar strong lensing systems with a 10-meter class telescope, we can examine the existence of dark microhaloes as the building blocks of dark matter structures. Failure to detect this signal may either be caused by a breakdown of cold dark matter (CDM) hierarchy on small scales, or rather interpreted as evidence against CDM paradigm, e.g. in favor of modified gravity models.

PACS numbers: 95.30.Sf, 98.62.Sb, 95.35.+d, 98.80.-k

## I. INTRODUCTION

The standard model of cosmology requires existence of cold dark matter (CDM) particles. The main role of CDM particles is to establish the gravitational skeleton of large scale structures [1]. An important statistical property of the dark matter structures is the power-spectrum of the structures which is predicted by e.g. the inflationary cosmology as one of the possible paradigms for the early universe [2]. The standard model of cosmology predicts nearly scale invariant, adiabatic and Gaussian distribution of matter at the early stages of the universe and the evolution of these structures strongly depend on the properties of the dark matter particles [3].

One of the predictions of CDM paradigm is the hierarchical structure formation, the existence of CDM substructures (from sub-haloes, down to microhaloes) embedded in the larger haloes [4]. The larger haloes host baryonic matter in the form of hot gas and stars at their centers. However, smaller haloes do not have enough

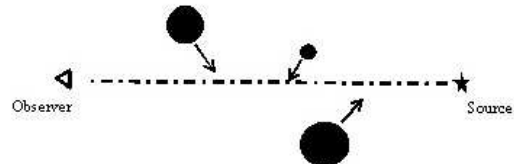


FIG. 1: The Dark Matter substructures moving relative to our line of sight towards a cosmological source.

gravitational potential to confine baryonic matter, hence microhaloes may not host any baryonic component.

An alternative to the dark matter paradigm is the modified gravity models, where the missing gravitational mass in the structures, and the universe, is compensated by the modification to the law(s) of gravity [5–7, 11]. Both dark matter and modified gravity models, at some level, can explain the rotation curves of the galaxies and formation of the structures [8–10]. However, it is hard to explain the whole range of observations, as the cluster of galaxies in Modified Newtonian Dynamics (MOND) [12] fails, while the Scalar-Tensor Vector Gravity (STVG) also so-called MOG can explain the dynamics of clusters in the context of baryonic matter [13].

The major efforts to test the existence of CDM particles have been performed in the underground experi-

\*Electronic address: [srahvar@pitp.ca](mailto:srahvar@pitp.ca)

†Electronic address: [baghram@ipm.ir](mailto:baghram@ipm.ir)

‡Electronic address: [nafshordi@pibt.ca](mailto:nafshordi@pibt.ca)

ments and null results from these experiments continue to push further constraints on the parameter space of the dark matter particles (e.g., [14, 15]). Similarly, the indirect searches for CDM are yet to result in conclusive evidence of its presence. While the main evidence for dark matter comes from its gravitational effect on large scales, different campaigns have studied its small-scale properties. One of the main efforts has been done by the gravitational microlensing experiments. These experiments monitor stars in the Large and Small Magellanic clouds and measured the magnification of stars by lensing. After a decade of observation, they could rule out dark matter in the form of massive compact objects in the halo, for nearly the entire range of viable astrophysical masses [16, 17]. Another proposal is astrometrical observation of the background stars by the lensing effect of the microhaloes [18]. The substructures in the parent halo can also modify the flux ratio of images in a strong lensing system [19]. The microhaloes may also change the pulsation time of the pulsars due to the Shapiro and Doppler effects [20].

Here, we propose yet another indirect gravitational method for the possible observation of the dark matter microhaloes, using the transient gravitational lensing on cosmological scales. In the dark matter scenario, the hierarchy of the structure formation predicts the existence of microhalo structures embedded in the larger haloes [4]. These structures have formed at high redshifts, and due to their small masses, have small virial velocity dispersions of  $\lesssim$  km/s. Due to the thermal pressure of the intergalactic medium, the baryonic matter cannot cool and condense into the gravitational potential of the microhaloes. The result is the formation of small non-baryonic structures, made of only the dark matter. In the case that these microhaloes cross our line of sight towards a cosmological source, such as a quasar, they could cause a slight change in the source flux due to the weak lensing effect. Unlike to the traditional weak lensing on the cosmological scales, the motion of the microhaloes provides a time varying magnification effect.

Let us make a simple estimate of the effect: Observations over a time period  $t$  are sensitive to microhaloes of the size  $r \sim vt$ , where  $v \sim 500$  km/s is the characteristic peculiar velocity on cosmological scales. Assuming the hierarchical structure formation scenario, we put all the mass of the universe in microhaloes of density  $\Delta\bar{\rho}_m$ , i.e.:

$$m = \bar{\rho}_m \times \Delta \times \frac{4}{3}\pi r^3. \quad (1)$$

If a typical microhalo forms at redshift  $z \sim 20$  (e.g. [22]), its density is enhanced by a factor of  $\sim 200$  due to collapse, and then diluted by a factor of  $\sim 0.03$  [23] due to subsequent tidal stripping, so we find  $\Delta \sim 20^3 \times 200 \times 0.03 \sim 10^5$ . The magnification by a single

microhalo at distance  $D$  is then given by:

$$\begin{aligned} \delta A_{\text{single}} &\sim 4\pi G \frac{m}{\pi r^2} \times D \sim (2\Omega_m H_0^2)(vt)D\Delta \\ &\sim 5 \times 10^{-9} \left(\frac{v}{500 \text{ km/s}}\right) \left(\frac{t}{1 \text{ yr}}\right) \left(\frac{\Delta}{10^5}\right) \left(\frac{D}{3 \text{ Gpc}}\right), \end{aligned} \quad (2)$$

where we assumed  $\Omega_m = 0.3$  and  $H_0 = 70$  km/s Mpc $^{-1}$ . This is clearly a tiny number! However, let us now estimate the optical depth, or the number of such microhaloes that cross the line of sight:

$$\begin{aligned} \tau &= \frac{\bar{\rho}_m}{m} \times \pi r^2 \times D \sim \frac{3D}{4vt\Delta} \\ &\sim 4 \times 10^7 \left(\frac{v}{500 \text{ km/s}}\right)^{-1} \left(\frac{t}{1 \text{ yr}}\right)^{-1} \left(\frac{\Delta}{10^5}\right)^{-1} \left(\frac{D}{3 \text{ Gpc}}\right). \end{aligned} \quad (3)$$

Therefore, the variance or noise in magnification due to the *collective* random contributions of many microhaloes becomes:

$$\begin{aligned} \delta A_{\text{tot.}} &= \sqrt{\tau} \delta A_{\text{single}} \sim \\ &3 \times 10^{-5} \left(\frac{v}{500 \text{ km/s}}\right)^{1/2} \left(\frac{t}{1 \text{ yr}}\right)^{1/2} \left(\frac{\Delta}{10^5}\right)^{1/2} \left(\frac{D}{3 \text{ Gpc}}\right)^{3/2}. \end{aligned} \quad (4)$$

This simple estimate illustrates the magnitude of the red stochastic photometric noise expected from transient weak lensing by millions of microhaloes that cross the line of sight to cosmological point sources. As we show in the paper, this effect could be magnified by as much as  $\sim 30$  for strongly lensed quasars, leading to variabilities of  $\delta A/A \sim 10^{-3}$  over months to years timescales. Moreover, the signal is expected to be close to gaussian, roughly to one part in  $\sqrt{\tau} \sim 10^4$  (from the central limit theorem), as it is contributed by many uncorrelated (and comparable) microhaloes. Therefore, temporal power spectrum should provide all the statistics necessary to quantify this noise.

One may worry that the cut-off of the CDM hierarchy is ignored in the above estimate, and no variation will be observed below a time-scale associated with this cut-off. In particular, the time-scale to cross the virial radius of a  $10^{-6} M_\odot$  microhalo that formed at  $z \sim 20$  is  $\sim 40$  years [63]. Nevertheless, even the smallest haloes are predicted to have a central cusp in the CDM paradigm, and thus their passage close to the line of sight can lead to rapid time-variations. For example, the cross-section for being within distance  $r < r_{\text{vir}}$  of a central cusp is  $\propto r^2$ , while the surface density for a singular isothermal profile is  $\Sigma \propto r^{-1}$ . Since  $\delta A_{\text{tot.}} = \sqrt{\tau} \delta A_{\text{single}}$ , these two effects exactly cancel each other. Simulated microhalo profiles are shallower in their center than singular isothermal (e.g.  $\Sigma \propto r^{-0.4}$  in [21]), which leads to a slight steepening of

the transient weak lensing noise below time-scales associated with the scale-radius of microhaloes. We further quantify this effect in Sec. III C.

In the rest of the paper, we present a precise formulation for the variability power spectrum in the lensing magnification, by assigning a velocity field to the perturbation of the metric perpendicular to our line of sight towards a given quasar. We do this calculation, both using the geodesic equation and using luminosity distance corrections to the focusing equation. Finally, we compare results with the present data from quasars and suggest an observational strategy for long term light curve measurement of quasars with high precision photometry.

The structure of paper is as follows: In Section II we use the perturbation theory in FRW and obtain fluctuations in the flux of quasar due to weak lensing of microhaloes on the cosmological scales. In Appendix A we repeat this calculation with the angular diameter distance formalism. We obtain the expected temporal power spectrum of the fluctuations of the light curve of a quasar for different non-linear models of structures in Section III. We then compare microhalo weak lensing signals with the intrinsic variation of quasar light and other backgrounds, such as stellar microlensing on the cosmological scales. In particular, we propose monitoring of multiply lensed quasar strong lensing systems as a way to distinguish the transient weak lensing effect from intrinsic variations. The conclusions are given in Section IV.

## II. TRANSIENT WEAK LENSING IN THE PERTURBED UNIVERSE: GEODESICS METHOD

In this section, we formulate the time variation of a source flux located at a cosmological distance, due to the lensing effect of DM substructures. We let the perturbations in the FRW metric move relative to the line of sight due to the peculiar velocity of structures and dispersion velocity of sub-structures embedded in a larger structure. Hence the transverse velocity produce a transient weak lensing effect and observationally the light curve of source can change with time.

We start with calculation of the geodesics equation of the light ray from the source to the observer. The perturbed FRW metric in the Newtonian gauge for the matter dominant era is given as below [24]:

$$ds^2 = -[1 - 2\Phi(\vec{x}, t)]dt^2 + a^2\delta_{ij}[1 + 2\Phi(\vec{x}, t)]dx^i dx^j, \quad (5)$$

where we set  $c = 1$ . The transverse spatial component of the light ray as well as the longitudinal direction follows the geodesics equation:

$$\frac{d^2 x^i}{d\lambda^2} + \Gamma_{\mu\nu}^i \frac{dx^\mu}{d\lambda} \frac{dx^\nu}{d\lambda} = 0, \quad (6)$$

where  $i$  is the index of the spatial coordinate and  $\lambda$ , the affine parameter is the comoving time measured by the

observers along the light ray. This affine parameter in the homogenous FRW universe is related to the coordinate time  $t$  and comoving distance  $\chi$  through the scale factor:

$$d\lambda = a dt = a^2 d\chi. \quad (7)$$

We assume a small transverse perturbation in the trajectory of the light rays compare to the longitudinal observer-lens and observer-source distances. Using the Christoffel symbols from metric in Eq.(5) and ignoring the higher orders of the perturbations, the geodesic equation simplifies to

$$\frac{d^2 x^i(\chi)}{d\chi^2} - 2\Phi_{,i} = 0, \quad (8)$$

where we replace the affine parameter with the comoving distance from Eq. (7). Now we change the transverse comoving coordinate with the angular position of the light ray to get the angular position of the source as function of angular position of images. Integrating Eq.(8), we obtain

$$\beta^i = \theta^i + \frac{2}{\chi_s} \int_0^{\chi_s} d\chi'' \int_0^{\chi''} \Phi_{,i}(\chi') d\chi', \quad (9)$$

where  $\beta^i$  is the angular position of the source,  $\theta^i$  is the observed angular position of the image and  $\chi_s$  is the comoving distance of the observer to the source. We simplify the double integral as

$$\beta^i = \theta^i + 2 \int_0^{\chi_s} \Phi_{,i}(\chi') \left(1 - \frac{\chi'}{\chi_s}\right) d\chi'. \quad (10)$$

The mapping matrix from the image space to the source space is given by

$$A_{ij} = \frac{\partial \beta^i}{\partial \theta^j} = \delta_{ij} + 2 \int \Phi_{,ij}(\chi') \left(1 - \frac{\chi'}{\chi_s}\right) \chi' d\chi'. \quad (11)$$

The Jacobian of transformation matrix in Eq.(11) within the framework of geometric optics provides the magnification by  $A = 1/\det(A_{ij})$ . For the low magnifications, ignoring higher order terms,  $A$  is given by

$$A \simeq 1 - 2 \int \nabla_{2D}^2 \Phi(\chi') \left(1 - \frac{\chi'}{\chi_s}\right) \chi' d\chi'. \quad (12)$$

We note that  $\nabla_{2D}^2$  is defined in two dimension lens plane, perpendicular to the line of sight. In the Fourier space  $\nabla_{2D}^2 \Phi(\chi', t)$  can be written as

$$\nabla_{2D}^2 \Phi(\chi', t) = - \int \frac{d^3 k}{(2\pi)^3} k_\perp^2 \Phi(k) e^{-ik_\perp \chi_\perp(t)} e^{-ik_\parallel \chi_\parallel}, \quad (13)$$

where  $k_\perp$  and  $k_\parallel$  are transverse and parallel wavenumbers. In writing Eq. (13), we use the so-called *moving sheet* approximation [20], where we assume the time dependence of the lensing potential is entirely due to the

coherent transverse motion of a lensing sheet. This approximation is justified as motion is dominated by cosmic velocities that are coherent on large scales. Therefore, in Eq. (13), only the transverse coordinate is a function of time,  $\chi_{\perp} = \chi_{\perp}(t)$ . Substituting Equation (13) in (12), the time variation of the magnification  $A$  obtained as:

$$\delta A(t) = 2 \int_0^{\chi_s} \left(1 - \frac{\chi'}{\chi_s}\right) \chi' d\chi' \times \int \frac{d^3 k}{(2\pi)^3} k_{\perp}^2 \Phi(k) e^{-ik_{\perp}\chi_{\perp}(t) - ik_{\parallel}\chi'}. \quad (14)$$

In Appendix A, we repeat this calculation and derive magnification variation based on the angular diameter

distance method. Now using this result, we investigate the statistics of magnitude variation as a function of duration of observation in the next section.

### III. CHARACTERISTICS OF QUASARS LIGHT CURVE: TRANSIENT WEAK LENSING

Imagine that we are measuring the light curve of a point like source at a cosmological distance. For an ideal quasar with stable light curve, we can define the correlation function in the magnification of the source due to the lensing by the microhaloes as follows:

$$\langle \delta A(t_1) \delta A(t_2) \rangle = 4 \int_0^{\chi_s} \left(1 - \frac{\chi''}{\chi_s}\right) \chi'' d\chi'' \int_0^{\chi_s} \left(1 - \frac{\chi'}{\chi_s}\right) \chi' d\chi' \int \frac{d^3 k}{(2\pi)^3} \frac{d^3 k'}{(2\pi)^3} \int \frac{v dv}{\sigma^2} (k_{\perp} k'_{\perp})^2 \langle \Phi(k, z) \Phi(k', z) \rangle \times \exp \left[ -ik_{\parallel}\chi' - ik'_{\parallel}\chi'' - v^2/2\sigma^2 - ivt_1 k_{\perp}/a - ivt_2 k'_{\perp}/a \right], \quad (15)$$

where  $t_1, t_2$  correspond to two subsequent observations with the interval of  $\tau = t_1 - t_2$  and  $v$  is the transverse velocity of substructures, which we have assumed to have a Maxwellian distribution and 1d dispersion velocity of  $\sigma$ . Here the transverse velocity is normalized to the cosmological scale factor to represent the velocity in the comoving space. We note that the peculiar velocity of the structures is a redshift and scale dependant parameter. Using the definition of the potential power spectrum:

$$\langle \Phi(\vec{k}, z) \Phi(\vec{k}', z) \rangle = (2\pi)^3 \delta^3(\vec{k} + \vec{k}') P_{\Phi}(\vec{k}, z), \quad (16)$$

and substituting in Eq.(15), we can integrate over  $k'$  for an ensemble of structures as follows:

$$\langle \delta A(t_1) \delta A(t_2) \rangle = 4 \int_0^{\chi_s} \left(1 - \frac{\chi''}{\chi_s}\right) \chi'' d\chi'' \int_0^{\chi_s} \left(1 - \frac{\chi'}{\chi_s}\right) \chi' d\chi' \int \frac{v dv}{\sigma^2} \int \frac{d^2 k_{\perp}}{(2\pi)^2} \frac{dk_{\parallel}}{2\pi} k_{\perp}^4 P_{\Phi}(\vec{k}, z) e^{-ik_{\parallel}(\chi' - \chi'')} e^{-i(t_1 - t_2)vk_{\perp}/a} e^{-v^2/2\sigma^2}. \quad (17)$$

Ignoring the longitudinal contribution in  $P(k, z)$  (i.e.  $k_{\perp} \gg k_{\parallel}$ ), and integrating over  $k_{\parallel}$  and  $\chi''$ , the correlation function simplifies to:

$$\langle \delta A(t_1) \delta A(t_2) \rangle = 4 \int_0^{\chi_s} \left(1 - \frac{\chi'}{\chi_s}\right)^2 \chi'^2 d\chi' \int \frac{v dv}{\sigma^2} \int \frac{dk_{\perp}}{2\pi} P_{\Phi}(k, z) k_{\perp}^5 e^{-ivk_{\perp}(t_1 - t_2)/a} e^{-v^2/2\sigma^2}. \quad (18)$$

In order to relate this correlation function with the observation, we replace the power spectrum in the potential with the density contrast, using the Poisson equation:

$$k^2 \Phi(k, z) = 4\pi G \rho_m(z) \delta(k, z) (1+z)^{-2}, \quad (19)$$

where  $\rho_m$  is the density of universe at redshift  $z$ . Using FRW equation, we can we write the Poisson equation as

$$\Phi(k, z) = \frac{3H_0^2 \Omega_m^0 (1+z)}{2k^2} \delta(k, z). \quad (20)$$

Consequently, the power spectrum of the potential in terms of dimensionless power-spectrum  $\Delta^2(k, z) = |\delta_k|^2 k^3 / 2\pi^2$  is given by

$$P_{\Phi}(k, z) = \frac{9\pi^2}{2k^7} H_0^4 \Omega_m^0 (1+z)^2 \Delta^2(k, z). \quad (21)$$

Substituting Eq.(21) in Eq.(18), correlation function of the light curve is given by

$$\langle \delta A(t_1) \delta A(t_2) \rangle = 18\pi^2 H_0^4 \Omega_m^0 (1+z)^2 \int_0^{\chi_s} \left(1 - \frac{\chi'}{\chi_s}\right)^2 \chi'^2 d\chi' \int \frac{v dv}{\sigma^2} \int \frac{dk_{\perp}}{2\pi} \frac{\Delta^2(k, z)}{k_{\perp}^2} (1+z(\chi'))^2 e^{-ik_{\perp}v(t_1 - t_2)/a} e^{-v^2/2\sigma^2}. \quad (22)$$

For structure with the size of  $k^{-1}a$ , a given transverse velocity of  $v$  implies the frequency of  $\omega = k_{\perp}v/a$  in the light curve. Replacing  $k_{\perp}$  with  $\omega$ , we use the definition of the temporal power spectrum as follows

$$\langle \delta A(t_1) \delta A(t_2) \rangle = \frac{1}{2\pi} \int P(\omega) e^{-i\omega\tau} d\omega, \quad (23)$$

where we replace  $\tau = t_1 - t_2$ . Then the dimensionless power spectrum of the light curve is given by

$$\omega P(\omega) = 18\pi^2 H_0^4 \Omega_m^{(0)2} \int_0^{\chi_s} \left(1 - \frac{\chi'}{\chi_s}\right)^2 \chi'^2 d\chi' \int_0^{\infty} dv e^{-v^2/2\sigma^2} \left[ \frac{v}{\sigma(\frac{\omega}{v}, z_{\chi'})} \right]^2 \frac{\Delta^2(\frac{\omega a}{v}, z_{\chi'})}{\omega} (1 + z_{\chi'})^3, \quad (24)$$

Here the power spectrum of magnification depends on distribution of DM which manifests itself by the matter power spectrum  $\Delta^2(k)$ . In order to calculate power-spectrum  $P(\omega)$ , corresponding to the light curve, we need a model for the evolution of velocity dispersion of DM substructures and the distribution of the matter in the small scales.

The velocity of CDM microhaloes results from the dispersion velocity in the galactic haloes, which in the host halo of typical galaxies  $\sigma \sim 200$  km/s, and from the bulk flow velocity in the intergalactic medium, that is  $\sigma \sim 500$  km/s [25, 26]. Now, in order to estimate the sensitivity of our observations to the scale of the relevant dark matter structures, we assume performing the light curve observations of a quasar from 1 day to 10 years. Assuming the corresponding velocities for the microhaloes, the time variation of quasar will probe nonlinear regime on the length scales of  $k \sim 10^8 - 10^{12}$  Mpc $^{-1}$ . These scales are significantly smaller than the reach of numerical simulations, or standard semi-analytical models (e.g. halo model) [27].

In the next subsection, we review the stable clustering hypothesis as a theoretical model for the small scale non-linear clustering of CDM (and its microhaloes). We then use this model to predict the amplitude of fluctuations in the quasar light curves due to transient weak lensing.

### A. Nonlinear matter power Spectrum: Stable Clustering in Phase Space

In this section we introduce the semi-analytical formalism of stable clustering in the phase space, along with other non-linear models of small scale clustering. The reason we require a semi-analytic model such as stable clustering is that numerical simulations can only explore the distribution of matter up to the scales of  $k \sim 10^3$  Mpc $^{-1}$  [28]. Moreover, currently there is no reliable observational constrains on the CDM power spectrum on sub-Mpc small scales.

The stable clustering model was first introduced by Davis & Peebles as an analytical method for calculating the correlation function of the structures in the deep non-linear regime [29]. In this model it is assumed that the

number of neighboring particles remains fixed. In other words, the pairwise velocity vanishes on small scales for non-linear structures. The idea was later extended to the phase space, where the number of particles in the vicinity of each point (i.e. fixed position and velocity) was assumed to not change with time [23, 30]. In the stable clustering hypothesis in phase space, for the small scales, the correlation function of densities is related to phase-space density as [20]:

$$\begin{aligned} \langle \rho(\vec{r}_i) \rho(\vec{r}_{ii}) \rangle &= \int d^3 \vec{v}_i d^3 \vec{v}_{ii} \langle f(\vec{r}_i, \vec{v}_i) f(\vec{r}_{ii}, \vec{v}_{ii}) \rangle \quad (25) \\ &\simeq \int d^3 \vec{v} d^3 \Delta \vec{v} \mu \langle f(\vec{r}, \vec{v}) \rangle \xi_s(\Delta r, \Delta v) \\ &= \mu \bar{\rho}_{avg} \int d^3 \Delta \vec{v} \cdot \xi_s(\Delta r, \Delta v). \end{aligned}$$

where  $f$  is the phase space density,  $\bar{\rho}_{avg}$  is the average density of matter and  $\mu$  is the fraction of dark matter substructure that survived tidal stripping.  $\xi_s$  is the phase space density of DM particles in the small volume of phase space ( $\Delta v$  and  $\Delta r$ ) obtained from spherical collapse results [31] and is related to the linear matter power spectrum through the variance of matter density (see [23] for a detailed calculations). For our study, we also need to know the matter power spectrum at different redshifts. Within the stable clustering hypothesis, the phase-space density  $\xi_s$  is assumed to be constant, and thus the evolution is simply given by the evolution of the background density. Hence the correlation function for the the small size non-linear overdensities can be written as:

$$\langle \delta(\vec{r}_i) \delta(\vec{r}_{ii}) \rangle \sim \frac{\mu}{\bar{\rho}_{avg}(1+z)^3} \int d^3 \Delta \vec{v} \cdot \xi_s(\Delta r, \Delta v). \quad (26)$$

In Fig.(2), we plot the dimensionless matter power-spectrum assuming stable clustering hypothesis in the phase space and  $\bar{\rho}_{avg} = \rho_{crit}$ . [64], where  $\mu = 0.1$  and the minimum mass of subhaloes is set to  $M_{DM} = 10^{-12} M_{\odot}$ . In Fig.(2), we also compare the fitting formula of Peacock and Dodds [32] (dash-dot-dot line) and the Halo model [33] (long dash line) for the non-linear power spectrum with the stable clustering. Now from the matter power spectrum and the assumption for the velocity dispersion of DM haloes we can compute the temporal power spectrum of quasar light curve.

We note that in Eq. (24), the velocity of structure is a combination of substructure velocity embedded in the halo and velocity of parent structure. Hence, the overall dispersion velocity is given by:

$$\sigma = (\sigma_{vir}^2 + \sigma_{halo}^2)^{1/2}, \quad (27)$$

where  $\sigma_{halo}$  is the dispersion velocity of parent halo which is determined through linear perturbation theory and  $\sigma_{vir}$  is the dispersion velocity of sub-haloes in parent halo. Assuming the spherical collapse model,  $\sigma_{vir}$  can be related to the mass of the parent halo as [34]:

$$\sigma_{vir} = 476g_\sigma(\Delta_{nl}E^2)^{1/6} \left( \frac{m}{10^{15}M_\odot/h} \right)^{1/3} km/s, \quad (28)$$

here  $g_\sigma = 0.9$ ,  $\Delta_{nl} = 18\pi^2 + 60x - 32x^2$  with  $x = \Omega_m - 1$ ,  $\Omega_m(z) = \Omega_m^0(1+z)^3$ ,  $E(z) = \Omega_m^0(1+z)^3 + \Omega_\Lambda$ . In the linear theory of structure formation,  $\sigma$  in Eq.(27) is related to linear matter power spectrum via

$$\sigma_{halo}(m, z) = Hf\sigma_{-1}\sqrt{1 - \sigma_0^4/\sigma_1^2\sigma_{-1}^2}, \quad (29)$$

where  $f \equiv d\ln\delta/d\ln a$  is the growth function and the linear moments of the dispersion velocity are defined by

$$\sigma_j^2(m) = \frac{1}{2\pi^2} \int dk k^{2+2j} P_m(k) W^2[kR(m)], \quad (30)$$

where  $W(x) = (3/x^3)[\sin(x) - x\cos(x)]$  is the Fourier transform of the spherical top-hat filter, and  $P_m(k)$  is the matter power spectrum. The dispersion velocity depends both on cosmology, the shape of power spectrum and the environment of the sub-halo. Using the dispersion velocity of sub-haloes and theoretical power spectrum in Fig.(2), we plot the dimensionless power spectrum of the magnification in equation (24) versus the frequency for various nonlinear models in Fig.(3).

For the stable clustering model, we also plot dimensionless power spectrum  $\omega P(\omega)$  for sources in various redshifts in Fig.(4). Increasing the redshift of source enhances the power spectrum of the light curve. Integrating over the power spectrum, we obtain the variance in the light curve within the window of  $\tilde{\omega} \in [\tilde{\omega}_0, \infty]$  which corresponds to  $T \in [0, T_0]$ ,

$$\sigma^2(\omega_0; z) = \frac{1}{2\pi} \int_{\omega_0}^{\infty} P(\omega) d\omega. \quad (31)$$

If  $T_{obs}$  is the duration of observations, then the longest observable mode is constrained by  $k^{-1} < vT_{obs}$  or  $\omega > T_{obs}^{-1}$ .

## B. Observational Target and Possible Backgrounds

Long term observations of quasars by the MACHO group [65] during the monitoring of Magellanic Clouds

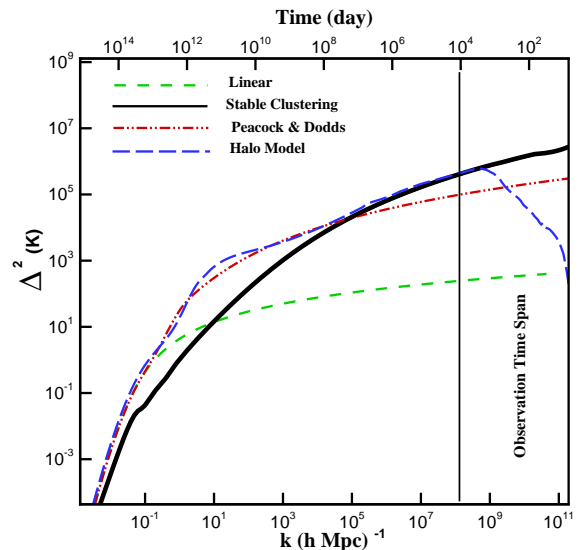


FIG. 2: Dimensionless power spectrum of density fluctuations  $\Delta^2(k) = k^3 P_{NL}(k)/(2\pi^2)$  as a function of wavenumber  $k$  for the linear regime (dashed line), Peacock and Dodds fitting formula (dash-dot-dot line), halo model (long-dashed line) and stable clustering hypothesis (solid line) with  $\mu = 0.1$

for detecting Massive Astrophysical Compact Halo Objects (MACHOs), provided a unique set of quasar light curves for duration of almost one decade [35]. They could report 47 quasars in the redshift range of  $0.2 < z < 2.8$  with sampling rate of 2 to 10 days. The COSMOGRAIL project is also an optical monitoring campaign that aims to measure time delays for a large number of gravitationally lensed quasars to accuracies of a few percent using a network of 1- and 2-m class telescopes [36]. The analysis of the light curves shows that the power spectrum of quasars follow a power law function as  $P(\omega) \propto 1/\omega^2$  [37]. This time variation of the quasar flux can be simulated by the autoregressive process. In this process each data point on the light curve relates to the next one by the equation of  $F_i = \alpha_{AR}F_{i-1} + \epsilon_i$ , where  $\epsilon_i$  is a normally distributed random variable with zero mean and variance of  $\sigma_{AB}$  and  $|\alpha_{AR}| < 1$  in order to ensure stationarity. The physics behind the variability of the quasar light curve is not clear, however it can be due to the disk instability [38], microlensing by the intervening stars [39] or due to the Poisson processes [40]. Recently the effect of dark matter haloes also has been studied in producing the caustic lines in the lens plane, making small magnification, short duration variations in the light curve [41].

The intrinsic variations of light can be removed if we use the time delay in the light curve of a quasar, lensed by an intervening galaxy or cluster of galaxies. The double or multiple images from the strong lensing enable us to find the time delay between the light curves of different images, and eventually intrinsic variations can be

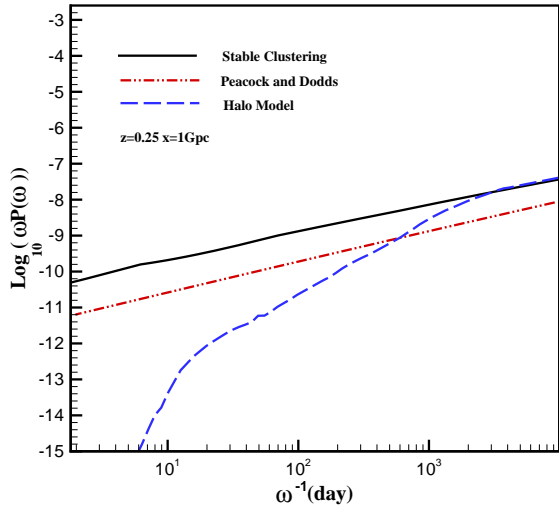


FIG. 3: Dimensionless power spectrum of magnification from Eq.(24) is plotted versus  $\omega^{-1}$ . The spectrum is plotted for stable clustering hypothesis (solid line) with  $\mu = 0.1$ , Peacock and Dodds fitting function (dashed-dotted line) and for halo model (long dashed line) with the cut-off related to the size of smallest halo mass of  $M_{min} = 10^{-6} M_{\odot}$ . Here the source is located at  $\chi = 1$  Gpc ( $z \sim 0.25$ ).

removed by time shifting [42]. While in principle with the time delay method one can remove the intrinsic variations, there are other intervening background signals from the microlensing events either by (i) stars intervening light bundles in the lensing galaxy [43] or (ii) stars belong to the galaxies distributed in the cosmological scales along our line of sight.

The strength of the microlensing signals depend on the column density of stars along our line of sight. We assume  $M_*$  as the mean mass of stars from the stellar mass function. The Einstein radius, which characterizes the size of a lens by star is given by

$$R_E = \sqrt{\frac{4GM_*}{c^2} \frac{\chi(z_l)\chi(z_l, z_s)}{\chi(z_s)}}, \quad (32)$$

where  $\chi(z_l)$ ,  $\chi(z_l, z_s)$  and  $\chi(z_s)$  are the distances of observer-lens, lens-source and observer-source in the co-moving frame. High density of stars on the lens plane can produce a network of caustic lines and crossing quasar with caustic lines produces strong magnifications in the quasar's light curve. However, the finite-size of quasar prevents singularities in the light curve and the caustic crossing of source just produce strong magnifications.

The transition from single occasional lensing to lensing by field of stars can be quantified by comparing the two dimensional number density of stars and the Einstein ring of individual stars. Assuming  $n_{2D}$  as the column number density of stars, in order to have single lensing regime, the

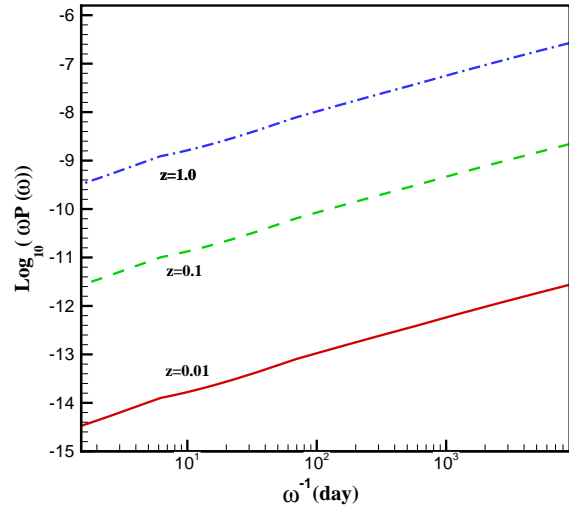


FIG. 4: Dimensionless power spectrum of magnification from Eq.(24) is plotted versus the frequency  $\omega^{-1}$  for sources at different redshifts (solid line for  $z=0.01$ , dashed line for  $z=0.1$  and dashed dot line for  $z=1$ ) for stable clustering model with  $\mu = 0.1$ .

relative distance between the lenses must be larger than the Einstein radius of lenses,  $n_{2D}^{-1/2} \gg R_E$ . Substituting the definition of Einstein radius from Equation (32), and using the definition of column density of stars, the condition of occasional single lensing regime implies  $\kappa \ll 1$  where  $\kappa = \Sigma(r)/\Sigma_{cr}$  and the critical column density is defined by

$$\Sigma_{cr} = \frac{c^2}{4\pi G} \frac{\chi(z_s)}{\chi(z_l)\chi(z_l, z_s)}. \quad (33)$$

In what follows we estimate the density of stars in the galactic halo and provide the condition for occasional microlensing events. For lens and source located at the cosmological scales (i.e.  $z \simeq 1$ ), we obtain a critical column density in the order of  $\Sigma_{cr} \simeq 10^3 M_{\odot} pc^{-2}$ . Now we assume a galactic halo around the lensing galaxy with isothermal density of

$$\rho(r) = \frac{M}{4\pi R} \frac{1}{r^2}, \quad (34)$$

where  $M$  is the mass of halo and  $R$  is the characteristic size of halo. Assuming a dark halo with a fraction of its mass made of MACHOs, we can relate the density of halo to the density of MACHOs as  $\rho_*(r) = f\rho(r)$  where from the microlensing experiments in the direction of Large and Small Magellanic Clouds, the upper bound of  $f$  is  $f < 0.2$  [44]. For the case of strong lensing with a Milky Way size galaxy,  $M = 5 \times 10^{11} M_{\odot}$  and  $R = 50$  kpc, we can calculate the convergence parameter corresponding

to the stars as

$$\kappa_\star = \frac{6 \times 10^{-3}}{h} \cos^{-1}(h), \quad (35)$$

where  $h$  is the position of images of quasars normalized to the size of halo (i.e.  $h = z/R$ ). For the case of  $h < 0.01$ ,  $\kappa_\star \simeq 1$  and we can detect the caustic crossing features from the network of caustic lines in the halo structure. Moreover, for the small impact parameters relative to the center of galaxy, the luminous parts of galaxy as disk and bulge also will contribute in the microlensing. For the outer regions of halo,  $h > 0.95$  the convergence parameter is  $\kappa_\star < 10^{-3}$  which is the favorable quasar lensing systems that form images around the Einstein ring. For a source, lens and observer aligned on a straight line, a Milky Way type galaxy as a lens on cosmological scales, equation (32) implies that Einstein ring forms at  $\simeq 10$  kpc. More massive galaxies or cluster of galaxies can make larger Einstein rings.

Recent analysis of quasar images in the SDSS catalog have found a sample of 26 lensed quasars brighter than  $I = 19.1$  and in the redshift range of  $0.6 < z < 2.2$ . These quasars are selected from 50,826 spectroscopically confirmed quasars in the SDSS Data Release 7 (DR7). For this sample of lensed quasars, the image separation ranges  $1'' < \theta < 20''$  where the I-band magnitude differences in two images is smaller than 1.25 mag [45]. This angular separation for the images in the cosmological scales corresponds to the spatial separation of images in the range of  $5 < L < 100$  kpc.

In some of quasar lensing systems, the lens is a cluster of galaxy with an extended halo. In this case, the situation is much better than lensing by a galaxy, as the haloes of clusters have much less MACHO densities, compared to the galactic haloes. However, the disadvantage of these systems is that the time delays between the distant images are longer, and a long-term survey of quasar's light curve for time-delay analysis is needed. The quasar SDSSJ1004+4112 belongs to this sample [46]. In this system, we have five images from the background quasar where some the images are close to the galaxies and exhibit microlensing features. Figure (5) demonstrate the lensing cluster and images from the background quasar. The apparent magnitude of images in red band for these images are:  $m_i(A) = 18.46 \pm 0.02$ ,  $m_i(B) = 18.86 \pm 0.06$ ,  $m_i(C) = 20.36 \pm 0.03$  and  $m_i(D) = 20.05 \pm 0.04$  [47]. The time ordering between the images are as C-B-A-D-E with the time delays of  $\Delta\tau_{BA} = 40.6 \pm 1.8$  days,  $\Delta\tau_{CA} = 821.6 \pm 2.1$  days,  $\Delta\tau_{CB} = 681 \pm 15$  days and  $\Delta\tau_{AD} > 1250$  days [48].

From the best model to the lensing system at the position of component A, the best values for the convergence and shear are  $\kappa = 0.392$  and  $\gamma = 0.642$  [49]. Similar to our arguments in the case lensing by a galaxy, images form at larger distances from the center of cluster have least contaminated by the stellar microlensing events [50].

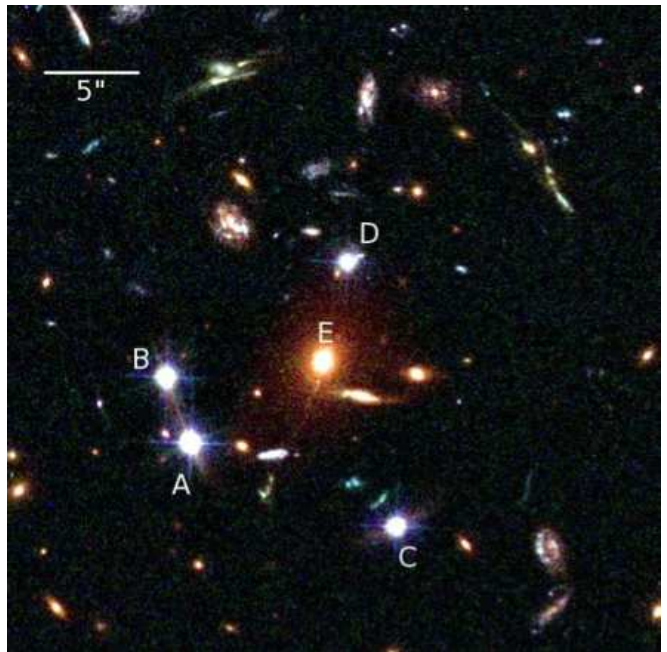


FIG. 5: SDSSJ1004+4112 strong lensing system as one of the exceptional lensing systems with images are split as large as 14.62 arcsec separation[46]. It seems that the lensing system is a cluster of galaxy with concentrated dark matter. The time delay between the images is of order a year. The apparent magnitude of images in red band are:  $m_i(A) = 18.46 \pm 0.02$ ,  $m_i(B) = 18.86 \pm 0.06$ ,  $m_i(C) = 20.36 \pm 0.03$  and  $m_i(D) = 20.05 \pm 0.04$  [47]. Photo adapted from [51] and by ESA, NASA, K. Sharon (Tel Aviv University) and E. Ofek (Caltech) .

Since most of the trajectory of light traveling from the source to the observer is in the intergalactic medium, there might also be microlensing events of cosmological origin as the background events. In order to estimate the probability of observation of the cosmological microlensing events, and their rate, we calculate the optical depth, or the probability that a background source is located inside the Einstein ring of a foreground (point) lens [53]:

$$\tau = \frac{4\pi G u_0^2}{c^2} \int \bar{\rho}_\star D_s^2 x(1-x) dx, \quad (36)$$

where  $\bar{\rho}_\star$  is the cosmological mean density of stars in the universe,  $u_0$  is the minimum impact parameter (size of lens) normalized to Einstein radius, and  $x = D_l/D_s$  is the ratio of the lens to the source distances. Using the Friedmann equation we can simplify expression (36) as

$$\tau \sim u_0^2 \Omega_\star (H_0 D_s)^2, \quad (37)$$

where  $\Omega_\star$  corresponds to the fraction of current cosmic density in stars, and  $H_0$  is the Hubble constant. For a quasar at cosmological distance  $D_s \sim H_0^{-1}$ . Using  $\Omega_\star \sim 10^{-2}$ , the optical depth for  $u_0 = 1$  (i.e.  $\mathcal{O}(1)$  magnification) assuming a uniform distribution of stars on cosmological scales, yields the optical depth of  $\tau \sim 10^{-2}$ .



A details analysis in [54], assuming that MACHOs follow dark matter content in the background and over-dense parts of university, confirms our estimated optical depth. This is also consistent with the studies of intracluster light, e.g. in [55], which find  $< 1\%$  of the cluster mass to be in the intracluster stars.

A realistic estimation for a lensing of a quasar by a galaxy can also be obtained by using the distribution function of the galaxies based on their size and number density, throughout the universe. Using the Press-Schechter distribution function [56], the optical depth of lensing of objects at the redshift of  $z_s \sim 2$  is about  $\tau \sim 10^{-2}$  [57] which is consistent with what we obtained from Equation (37).

While it is reassuring that microlensing events that lead to  $> \mathcal{O}(1)$  magnification are not common, it is clear that magnification events of  $\sim 10^{-4}$  have higher optical depth. The low magnification in the microlensing events is given by  $\propto (\theta_E/\theta)^4$  in the field, and  $\propto (\theta_E/\theta)^2$  in strongly lensed systems, as function of the angular separation  $\theta$ , between the quasar and the star. Therefore, events with  $\theta \sim 10 \times \theta_E$  would have optical depth of unity, implying that magnifications of  $10^{-4}$  ( $10^{-2}$ ) are common in the field (strongly lensed systems). However, the characteristic time-scale for microlensing events of this size is given by:

$$t(\theta) \sim \frac{\theta}{\theta_E} \sim \left( \frac{\theta}{\theta_E} \right) \left( \frac{R_E}{v} \right) = (230 \text{ yr}) \left( \frac{\theta/\theta_E}{10} \right) \left( \frac{M_*}{M_\odot} \right)^{1/2} \left( \frac{\chi(z_s)}{3 \text{ Gpc}} \right)^{1/2} \left[ \frac{v(\text{km/s})}{500} \right]^{-1}, \quad (38)$$

assuming that the typical lens is half-way to the source. Therefore, we see that the characteristic time-scales for typical magnification events (i.e. with  $\tau \gtrsim 1$ ) is quite long, and thus they are unlikely to contaminate the transient weak lensing due to microhaloes. In Appendix B, we derive the power spectrum of weak stellar microlensing light curves, and show that they are suppressed by  $\exp[-2t(\theta)/T_{obs}]$ , which is shown in Fig. (6) for the nominal parameters in Eq. (38).

In denser fields, it is more likely to find a star close to the line of sight, so that  $\exp[-2t(\theta)/T_{obs}]$  is not too small. In such cases, the main microlensing signal will be dominated by the handful of stars within the radius  $\theta T_{obs}$ . Given the small number of lenses, the statistics of the signal will be very non-gaussian, with significant phase correlation among different Fourier amplitudes, as well as a sharp exponential drop at high frequencies (see Fig. 6). This will be in contrast with the transient weak lensing due to microhaloes, which (as we argued in Sec. I) is almost perfectly gaussian, and nearly power-law in frequency  $P(\omega) \propto \omega^{-1.69}$  (e.g. Fig. 4).

### C. Present observations and prospects: Case study for SDSSJ1004+4112

In order to measure the light curve of a source with a given photometric precision, we use the definition of the signal to noise ratio in each data point due to deviation with respect to the base line by  $Q_i = \delta A_i L_i / \sigma_L$ , where  $L_i$  is the luminosity at  $i$ th point and  $\sigma_L$  is the corresponding error bar. The variance of the signal to noise can be obtain by  $\sqrt{\langle Q^2 \rangle} = \sqrt{\langle \delta A^2 \rangle} \bar{L} / \sigma_L$ . In order to have signal to noise larger than a given threshold, the error bar should satisfy in the following constraint

$$\frac{\sigma_L}{\bar{L}} < \frac{\sqrt{\langle \delta A^2 \rangle}}{Q_{min}}. \quad (39)$$

For a given source with the rate of  $\beta$  photons per second received by the telescope, the number of collected photons is  $L = \beta T_{exp}$ . Considering photometric error due to the Poisson fluctuations, the left hand side of equation (39) can be written as  $(\beta T_{exp})^{-1/2}$ , where the rate of photons received by a telescope is given by  $\beta = \frac{F}{\langle h\nu \rangle} \pi (D/2)^2$ . Then the essential exposure time  $T_{exp}$  to achieve a minimum signal to noise of  $Q_{min}$  is given by:

$$T_{exp} > \frac{Q_{min}^2}{\langle \delta A^2 \rangle} \frac{\langle h\nu \rangle}{F_0} \frac{4}{\pi D^2} 10^{\frac{m-m_0}{2.5}}. \quad (40)$$

Here we use the flux and magnitude of the Sun as reference with the absolute magnitude of  $m_0 = 4.75$  and corresponding photon flux of  $F_0 / \langle h\nu \rangle = 8.3 \times 10^8 \text{ m}^{-2} \text{ sec}^{-1}$ . For a small size telescope with the diameter of  $D = 1.54 \text{ m}$  (as Danish Telescope at La Silla), the minimum exposure time for a star with the magnitude of  $m$ , having an average signal to noise ratio larger than three, is obtain by

$$T_{exp}(D = 1.54) > 6.3 \times 10^{-10} \times 10^{\frac{m-4.75}{2.5}} \frac{Q_{min}^2}{\langle \delta A^2 \rangle} \text{sec}. \quad (41)$$

For the case of strong lensing images of SDSSJ1004+4112, we use the redshift of source at  $z_s = 1.734$  [47]. Also, using the convergence and shear for the lensing clustering as  $\kappa = 0.392$  and  $\gamma = 0.642$  [49], we obtain the overall magnification for transient weak lensing using:

$$\frac{\delta A}{A_0} \simeq \frac{2(\kappa^2 + \gamma^2)^{1/2} \delta A_{int}}{|(1 - \kappa)^2 - \gamma^2|} \simeq 35 \times \delta A_{int}. \quad (42)$$

Here the magnification factor due to strong lensing is  $A_0 = |(1 - \kappa)^2 - \gamma^2|^{-1} \sim 23.5$ , and  $\delta A_{int}$  is the transient magnification, due to microhaloes, in the absence of the strong lens. Figure (6) represents variance in the light curve of the Quasar from the transient weak lensing in terms of period of modes for two models of stable clustering, and Halo model fitting function. The variance in

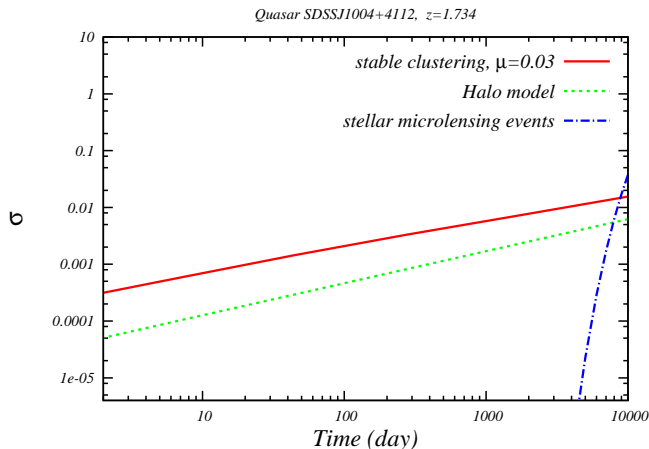


FIG. 6: The expected standard deviation of the magnification due to the transient weak lensing in the light curve of SDSSJ1004+4112 from one day up to  $10^4$  days. The standard deviation is obtained for the stable clustering (solid line) with  $\mu = 0.03$ , halo model fitting function (dotted line) with the cut-off of  $M_{min} = 10^{-6} M_{\odot}$ . The expected signal from a typical cosmological microlensing event is also shown for comparison (dot-dashed curve; see Appendix B).

the fluctuation of the light curve depends on the cutoff on the mass of microhalos. This cutoff in the mass is a function of micro-physics of dark matter particles that determines the size of free stream mass scale. Recent simulations provides the profile of the abundant microhalos [60] for the earth mass halos. In order to study the effect of cutoff mass of microhalos on transient weak lensing effect, we plot the variance in the light curve of the Quasar as a function time scale for three cases of cutoff masses in Figure (7). Smaller cutoff results in larger variance in the variation of light curve by the transient weak lensing.

To achieve a  $3\sigma$  signal to noise ratio, a variation in magnification of  $\sim 2 \times 10^{-3}$  (which occur e.g. over a hundred days within the stable clustering model), Equation (41) implies

$$T_{exp}(D = 1.54) > 1.14 \times 10^{\frac{m-7.75}{2.5}} \text{sec}. \quad (43)$$

For the case of this Quasar, the magnitude of images are in the order of  $m \simeq 18.5$ , substituting in equation (43), we get the exposure time of  $T_{exp}(D = 1.54) > 2 \times 10^4$  sec. Increasing the diameter of telescope reduces the exposure time as  $T_{exp} \propto 1/D^2$ . For a 10-meter class telescope, the exposure time reduces by the factor of 0.023 and we get the exposure time of  $T_{exp}(D = 10) > 500$  sec. Repeating this calculation for the halo model, which has a smaller standard deviation by an order of magnitude compared the stable clustering model, we would expect that exposure time for detecting signal has to be two orders of magnitudes larger, i.e.  $T_{exp}(\text{halo model}) \sim 10^2 \times T_{exp}(\text{stable clustering})$ .

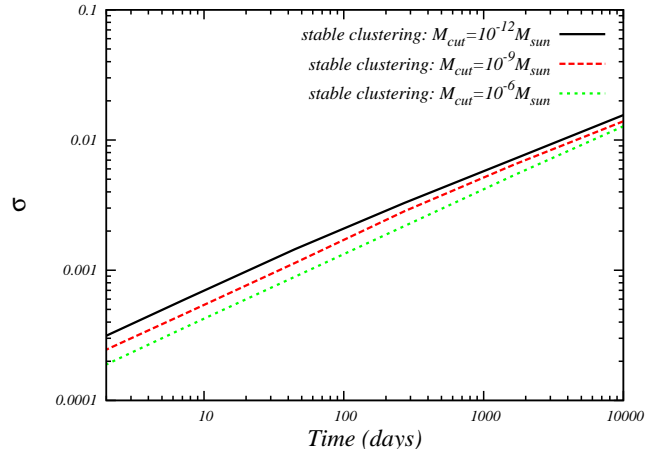


FIG. 7: Same as Fig. (6), but for different cutoff masses in the stable clustering model. Smaller cutoff provides larger variation in the light curve as the variance receives contribution from smaller haloes. This is a more significant effect for shorter time-scales, which are sensitive to smaller haloes.

From the technical point of view, we can achieve higher photometric accuracy with long term exposures even with the same size telescopes. One of the problems with the long exposure times is that CCD may saturate during the photometry. This problem can be solved by telescope defocusing technique, which is widely used in the transit exoplanet observations [61]. Another solution is that images can be taken with shorter exposures, then stack to get a desired signal to noise ratio.

#### IV. CONCLUSION

In this work, we propose the possibility of observation of transient weak lensing of quasars, as a probe of the microhaloes on the cosmological scales. These observations can rule out the existence of dark microhaloes or constrain the properties of the dark matter particles, as well as the models of non-linear structure formation. Assuming different models for non-linear structures on small scales, we formulate the weak lensing of the microhaloes by the geodesic and angular distance methods. We note that, due to weak gravitational potential of these structures they don't host baryonic/stellar matter in their centers.

The transient weak lensing signal is caused by random contributions of millions of microhaloes, and thus yields an almost perfect gaussian photometric noise. We obtained the temporal power spectrum of this photometric noise in the light curve, finding a near power-law red spectrum of  $P(\omega) \propto \omega^{-1.69}$ . For the quasar strong lensing systems, the variation in the light curve due to transient weak lensing can be of the order of  $10^{-4} - 10^{-3}$ , depending on the halo models.

In contrast, the intrinsic variations of quasar light can be as much as an order of magnitude. However, we have argued that, in principle, we can separate the intrinsic variation of quasars from the transient weak lensing by the time delay method for multiple images in a strong lensing systems. Moreover, we showed that the primary contamination of this signal by stellar microlensing can be effectively cleaned, as it has a significantly different amplitude, statistics, and frequency dependence.

Finally, for the observation of transient weak lensing we proposed monitoring images of quasars in a strong lensing system, preferably lensed with a cluster of galaxies. Amongst bright lensed Quasars in the SDSS Data Release 7, SDSSJ1004+4112 is lensed by cluster of galaxy with images formed at large angle separation. The advantage of using strong lensing system is that (i) we can remove the intrinsic variations of a quasar by time delay method and (ii) the transient weak lensing signals can be enhanced by the magnification of the source due to the strong lensing. For the case of stable clustering, we calculated an exposure time of  $\sim 500$  sec with a 10-meter class telescope to achieve  $3\sigma$  signal to noise ratio in detection of time variation by the transient weak lensing. A long term monitoring of this system is therefore proposed as

a means to study the nature of dark matter microhaloes on the cosmological scales. The result of observations, either will constrain the existence of microhaloes, or rule them out as the building blocks of dark matter structures in favour of modified gravity alternatives, or more conservatively, a breakdown in CDM hierarchy on small scales.

### Acknowledgments

We would like to especially thank Avery Broderick for reminding us about the power of multiple-image strong lensing for differentiating our signal from intrinsic quasar variability. We would also like to thank Adrienne Erickcek, Neal Dalal, and James Taylor for invaluable discussions and/or feedback on the manuscript. This research was supported by Perimeter Institute for Theoretical Physics and the John Templeton Foundation. Research at Perimeter Institute is supported by the Government of Canada through Industry Canada and by the Province of Ontario through the Ministry of Economic Development & Innovation.

- 
- [1] C. S. Frenk, S. D. M. White and , “Dark matter and cosmic structure,” *Annalen Phys.* **524**, 507 (2012) [arXiv:1210.0544 [astro-ph.CO]].
- [2] A. H. Guth, “The Inflationary Universe: A Possible Solution To The Horizon And Flatness Problems,” *Phys. Rev. D* **23**, 347 (1981); K. Sato, “First Order Phase Transition of a Vacuum and Expansion of the Universe,” *Mon. Not. Roy. Astron. Soc.* **195**, 467-479 (1981). A. D. Linde, “A New Inflationary Universe Scenario: A Possible Solution Of The Horizon, Flatness, Homogeneity, Isotropy And Primordial Monopole Problems,” *Phys. Lett. B* **108**, 389 (1982); A. Albrecht and P. J. Steinhardt, “Cosmology For Grand Unified Theories With Radiatively Induced Symmetry Breaking,” *Phys. Rev. Lett.* **48**, 1220 (1982).
- [3] S. Dodelson, *Modern Cosmology*, Academic Press (2003)
- [4] Moore, B., Ghigna, S., Governato, F., et al., *Astrophysical Letter* 524, L19 (1999).
- [5] M. Milgrom, *ApJ*, 270, 365 (1983).
- [6] J. W. Moffat, *JCAP* 3, 4 (2006).
- [7] J. D. Bekenstein, *Phys Rev D*, 70, 083509 (2004).
- [8] Begeman, K. G., Broeils, A. H., & Sanders, R. H. *MNRAS*, 249, 523 (1991).
- [9] J. R. Brownstein and J. W. Moffat, *ApJ* 636, 721 (2006)
- [10] Y. Sobouti, *A&A*, 464, 921 (2007); S. Rahvar, & Y. Sobouti, *Modern Physics Letters A* 23, 1929 (2008)
- [11] J. W. Moffat & S. Rahvar, *MNRAS* **2316** ( 2013)[arXiv:1306.6383]
- [12] G. W. Angus, B. Famaey & H. S. Zhao, *MNRAS* 371, 138 (2006).
- [13] J. W. Moffat & S. Rahvar, arXiv:1309.5077
- [14] G. Bertone, D. Hooper, J. Silk and , “Particle dark matter: Evidence, candidates and constraints,” *Phys. Rept.* **405**, 279 (2005) [hep-ph/0404175].
- [15] P. Beltrame [on behalf of the XENON Collaboration], arXiv:1305.2719 [astro-ph.CO].
- [16] A., Milsztajn & T. Lasserre., 2001, *Nuclear Physics B Proceedings Supplements*, 91, 413
- [17] Alcock, C., Allsman, R. A., Alves, D. R., et al. 2000, *ApJ*, 542, 281
- [18] A. L. Erickcek & N. M. Law, *ApJ* 729, 49 (2011)
- [19] R. B. Metcalf & H. Zhao, *ApJ* **567**, L5 (2002); N. Dalal and C. S. Kochanek, *ApJ* **572**, 25 (2002); J. P. McKean et al. *MNRAS* **378**,109 (2007)
- [20] S. Baghran, N. Afshordi, K. M. Zurek *Phys. Rev. D* **84**, 043511 (2011), arXiv:1101.5487
- [21] D. Anderhalden and J. Diemand, *JCAP* **1304**, 009 (2013) [Erratum-ibid. **1308**, E02 (2013)] [arXiv:1302.0003 [astro-ph.CO]].
- [22] R. E. Angulo and S. D. M. White, *Mon. Not. Roy. Astron. Soc.* **401**, 1796 (2010) [arXiv:0906.1730 [astro-ph.CO]].
- [23] N. Afshordi, R. Mohayaee and E. Bertschinger, *Phys. Rev. D* **81**, 101301 (2010).
- [24] J. M. Bardeen, *Phys. Rev. D* 22, 1882 (1980)
- [25] A. Abate and H.A. Feldman, *Mon. Not. Roy. Astron. Soc.* **419** 3482 (2011).
- [26] R.K. Sheth and A. Diaferio, *Mon. Not. Roy. Astron. Soc.* **322**, 901.
- [27] C. -P. Ma, J. N. Fry and , “Deriving the nonlinear cosmological power spectrum and bispectrum from analytic dark matter halo profiles and mass functions,” *Astrophys. J.* **543**, 503 (2000) [astro-ph/0003343].
- [28] M. Bolyan-Kolchin, *et al.*, *Mon. Not. Roy. Astron. Soc.*

- 398**, 1150, (2009).
- [29] M. Davis and P. J. E. Peebles, , ApJS **34**, 425 (1977).
- [30] J. Zavala and N. Afshordi, arXiv:1308.1098 [astro-ph.CO].
- [31] J. E. Gunn and J. R. Gott, III, “On the Infall of Matter into Clusters of Galaxies and Some Effects on Their Evolution,” *Astrophys. J.* **176**, 1 (1972).
- [32] J. A. Peacock & S. J. Dodds, *Mon. Not. Roy. A. Soc.* **280**, L19 (1996).
- [33] R.E. Smith et al., *Mon. Not. Roy. A. Soc.* **341**, 1311 (2003).
- [34] Bryan, G. L., Norman, M., *ApJ*, **495**, 80 (1998)
- [35] M. Geha, et al. *AJ*, **125**, 1 (2003)
- [36] F. Courbin, V. Chantry, Y. Revaz, et al., *A&A* **536**, A53 (2011); C. Vuissoz, F. Courbin, D. Sluse, et al. *A&A* **488**, 481 (2008); C. Vuissoz, F. Courbin, D. Sluse, et al., *A&A* **464**, 845 (2007)
- [37] B. C. Kelly, J. Bechtold, and A. Siemiginowska, *AJ* **698**, 895, (2009)
- [38] T. Kawaguchi, S. Mineshige, M. Umemura & E. L. Turner, *ApJ*, 504, 671 (1998).
- [39] R. W. Schmidt & J. Wambsganss, *General Relativity and Gravitation*, 42, 2127 (2010).
- [40] R. Cid Fernandes, L., Jr. Sodre & L., Jr. Vieira da Silva, *ApJ* 544, 123 (2000).
- [41] J. Chen & S. M. Koushiappas, *ApJ* 724, 400 (2010)
- [42] I. Burud, J. Hjorth, F. Courbin, et al., *A&A*, 391, 481 (2002).
- [43] J. Wambsganss, B. Paczynski and P. Schneider, *ApJ* **358L**, 33 (1990).
- [44] T. Lasserre, C. Afonso, J. N. Albert, et al. *A&A*, 355, L39
- [45] N. Inada, M. Oguri, M. Shin, et al. *ApJ*, 143, 15 (2012)
- [46] N. Inada et al., *Nature* 426, 810 (2003)
- [47] Oguri, M., Inada, N., Keeton, C. R., et al., *ApJ*, 605, 78 (2004)
- [48] J. Fohlmeister, C. S. Kochanek, E. E. Falco, C. W. Morgan, and J. Wambsganss, *ApJ*, 676, 761 (2008); J. Fohlmeister et al. *ApJ*, 662, 62 (2007)
- [49] T. Gordon et al. *ApJ*, 610, 679 (2004)
- [50] G. T. Richards, C. R. Keeton, B. Pindor et al., *ApJ*, 610, 679 (2004)
- [51] Oguri, M., *Publ. Astron. Soc. Japan* 62, 1017, (2010)
- [52] Q. Yu, & S. Tremaine, *ApJ*, 599, 1129 (2003).
- [53] B. Paczynski, *ApJ* **304**, 1 (1986)
- [54] E. Zackrisson & T. Riehm *A&A* **475**, 453 (2007)
- [55] J. M. Budzynski, S. E. Kposov, I. G. McCarthy and V. Belokurov, arXiv:1309.1183 [astro-ph.CO].
- [56] W. H. Press & P. Schechter, *ApJ*, 187, 425 (1974)
- [57] R. Barkana & A. Loeb, *ApJ* 531 613 (2000)
- [58] P. Schneider, J. Ehlers and E.E. Falco, *Gravitational Lenses*, Springer (1992)
- [59] M. Schmidt and R. F. Green, *ApJ* 269, 352 (1983)
- [60] D. Anderhalden & J. Diemand, *JCAP*, 4, 9 (2013)
- [61] J. Southworth et al. *A&A* 527, 8 (2011)
- [62] C. Vanderriest, J. Schneider, G. Herpe et al. 1989, *A&A*, 215, 1
- [63] We thank James Taylor for bringing this point to our attention.
- [64] In the case of microhaloes in a background parent halo,  $\bar{\rho}_{avg}$  should be the density of the halo that hosts the microhaloes
- [65] <http://www.macho.anu.edu.au>

## Appendix A: Transient Weak Lensing: Angular Diameter-Distance method

For a bundle of light rays emitting from a source, the relative change on the surface of light bundle in a generic metric is given by

$$\frac{dA}{Ad\lambda} = 2\theta = k^\mu{}_{;\mu}, \quad (\text{A1})$$

where  $k^\mu$  is the tangent vector to the null geodesics and  $\theta$  represents the isotropic contraction and expansion of the light beam. The equation governs the dynamics of  $\theta$  and shear is given by [58]:

$$\theta' + \theta^2 + |\sigma|^2 = -\frac{1}{2}R_{\mu\nu}k^\mu k^\nu, \quad (\text{A2})$$

where  $\prime$  stands for derivative with respect to the affine parameter and  $|\sigma|$  is the magnitude of shear tensor define as below:

$$|\sigma|^2 = \frac{1}{2}k_{\mu;\nu}k^{\mu;\nu} - \frac{1}{4}(k^\alpha{}_{;\alpha})^2. \quad (\text{A3})$$

Combining equations (A1) and (A2) results in the focusing equation

$$\sqrt{A}'' = -(|\sigma|^2 + \frac{1}{2}R_{\mu\nu}k^\mu k^\nu)\sqrt{A}. \quad (\text{A4})$$

This equation can be used for studying the influence of matter on the light bundle while it propagates from the source to the observer. The effect of matter distribution relates to the Ricci tensor and the magnitude of shear tensor. The components of Ricci tensor from the metric in equation (5) is given by [3]:

$$R_{00} = -3\frac{\ddot{a}}{a} - a^{-2}\nabla^2\Phi - \ddot{\Phi} + 6H\dot{\Phi}, \quad (\text{A5})$$

and

$$R_{ij} = \delta_{ij} \left[ (2a^2H^2 + a\ddot{a})(1 + 4\Phi) + 7a^2H(\dot{\Phi}) + a^2\ddot{\Phi} - \nabla^2\Phi \right], \quad (\text{A6})$$

where “ $\cdot$ ” is derivative with respect to coordinate time,  $t$ . For solving the focusing equation we replace the  $k^\mu = dx^\mu/d\lambda$  with the observable parameters. Here  $\lambda$  is defined similar to Eq.(7). We set  $\lambda$  to zero at the position of the observer and the final value at the location of the source, then  $adt = a^2d\chi = -d\lambda$  and  $k^\mu$  in FRW metric can be given by:

$$\begin{aligned} k^\mu &= (-a^{-1}, -a^{-2}, 0, 0), \\ k_\mu &= (a^{-1}, -1, 0, 0). \end{aligned} \quad (\text{A7})$$

On the other hand the Ricci term in Eq.(A4) is obtained as

$$\frac{1}{2}R_{\mu\nu}k^\mu k^\nu = \frac{4\pi G\rho}{a^2} + \frac{16\pi G\rho}{a^2}\Phi - \frac{1}{a^4}\nabla^2\Phi - \frac{\ddot{\Phi}}{a^2} - \frac{H\dot{\Phi}}{a^2}, \quad (\text{A8})$$

For the shear term we need to calculate the following elements:

$$k_{\mu;\nu}k^{\mu;\nu} = k_{0;0}k^{0;0} + k_{i;0}k^{i;0} + k_{0;i}k^{0;i} + k_{i;j}k^{i;j} \quad (\text{A9})$$

where  $i, j$  represent spatial components and

$$k_{0;0}k^{0;0} = \left(\frac{H}{a}\right)^2 + \frac{2H}{a^2}(-\dot{\Phi} + \frac{\Phi_{,x_{||}}}{a}), \quad (\text{A10})$$

$$k_{i;0}k^{i;0} = k_{0;i}k^{0;i} = -\left(\frac{H}{a}\right)^2 - 2Ha^{-2}(\dot{\phi} + a^{-1}\Phi_{,x_{||}}),$$

$$k_{i;j}k^{i;j} = 3\left(\frac{H}{a}\right)^2 + 24\left(\frac{H}{a}\right)^2\Phi + 6\frac{H\dot{\Phi}}{a^2} + \frac{2}{a^3}H\Phi_{,x_{||}},$$

Substituting in equation (A3), the shear term obtain as follows:

$$|\sigma|^2 = 12\left(\frac{H}{a}\right)^2\Phi - \frac{2H\dot{\Phi}}{a^2} - \frac{2H}{a^3}\Phi_{,x_{||}}. \quad (\text{A11})$$

Finally, substituting Equations (A8) and (A11) in focusing equation and changing the affine derivatives to the coordinate time derivatives, we get:

$$\ddot{D} - H\dot{D} + 4\pi\rho GD + \mathcal{F}D = 0, \quad (\text{A12})$$

where we rename  $D \equiv \sqrt{A}$ , representing the angular diameter distance to any point at the light bundle and  $\mathcal{F}$  is given by:

$$\mathcal{F} = 15H^2\Phi - 3H\dot{\Phi} - a^{-2}\nabla^2\Phi - \ddot{\Phi} - 2Ha^{-1}\Phi_{,x_{||}}. \quad (\text{A13})$$

Note that some of these terms with the factor of  $H^{-1}$  represent variation of the perturbation during the Hubble time scale, some terms with the partial derivative with respect to the time  $\partial_t$  represent intrinsic time variation of the perturbations and some terms with  $\partial_x$  represents the spatial variation of the field. In order to get a differential equation for perturbation of  $D$ , we write the angular diameter distance as sum of  $D_0$  due to the unperturbed FRW and the first order perturbation term  $D_1$ :

$$D = D_0 + D_1. \quad (\text{A14})$$

The background evolution and the first order perturbation can be divided into two equations as:

$$\ddot{D}_0 - H\dot{D}_0 + 4\pi G\rho D_0 = 0, \quad (\text{A15})$$

$$\ddot{D}_1 - H\dot{D}_1 + 4\pi G\rho D_1 + \mathcal{F}D_0 = 0, \quad (\text{A16})$$

where the solution of Eq. (A15) in terms of the comoving distance is  $D_0 = a\chi$ . To solve the Eq.(A16), we assume that the time variation due to the motion and spatial gradient of substructures is smaller than the Hubble time scale

$$\Delta x/c, t_{DM} \ll t_{Hubble}, \quad (\text{A17})$$

hence  $H\dot{\Phi} \ll \ddot{\Phi}$ ,  $H^2\Phi \ll \ddot{\Phi}$ ,  $H/a\Phi_{,x_{||}} \ll \ddot{\Phi}$  and Eq.(A16) reduces to:

$$\ddot{D}_1 - \left[\ddot{\Phi} + a^{-2}\nabla^2\Phi(x, t)\right]D_0 = 0. \quad (\text{A18})$$

We use Fourier transform for  $\Phi$  and consider a transverse velocity for the perturbation as  $x_{\perp} \rightarrow x_{\perp} + \frac{v_{\perp}t}{a}$ . Hence time derivative of  $\Phi$  is given by

$$\ddot{\Phi}(\chi, t) = - \int \frac{d^3k}{(2\pi)^3} \left(\frac{k_{\perp}v}{a}\right)^2 \Phi(k) e^{-ik_{||}\chi_{||}} e^{-ik_{\perp}x_{\perp}(t)}, \quad (\text{A19})$$

and for the gradient of perturbation we have

$$\frac{1}{a^2}\nabla^2\Phi(\chi, t) = - \int \frac{d^3k}{(2\pi)^3} \frac{k_{\perp}^2 + k_{||}^2}{a^2} \Phi(k) e^{-ik_{||}\chi_{||}} e^{-ik_{\perp}x_{\perp}(t)}. \quad (\text{A20})$$

Assuming that  $v \ll 1$ , we can ignore the time derivative term of  $\Phi$ , then Eq.(A18) reduces to

$$\ddot{D}_1(t) = -D_0(t) \int \frac{d^3k}{(2\pi)^3} \frac{k_{\perp}^2 + k_{||}^2}{a^2} \Phi(k) e^{-ik_{||}\chi_{||}} e^{-ik_{\perp}x_{\perp}(t)}. \quad (\text{A21})$$

For a perturbed FRW metric in flat universe, the angular diameter distance can be written as  $D = a(\chi + \epsilon(\chi))$ , where  $\epsilon(\chi)$  is the first order perturbation in terms of comoving distance and  $D_1 = a\epsilon(\chi)$ . Hence the perturbation in the luminosity distance along the propagation of the light can be written as:

$$\ddot{D}_1 = \frac{1}{a} \frac{d^2\epsilon(\chi)}{d\chi^2}. \quad (\text{A22})$$

Consequently equation(A22) can be written as:

$$\epsilon(\chi) = - \int \frac{d^3k}{(2\pi)^3} (k_{\perp}^2 + k_{||}^2) \Phi(k) e^{-ik_{\perp}\chi_{\perp}} \int_0^{\chi_s} d\chi' \int_0^{\chi'} e^{-ik_{||}\chi''} \chi'' d\chi''. \quad (\text{A23})$$

We can simplify this integral as

$$\epsilon(\chi) = -\chi_s \int \frac{d^3k}{(2\pi)^3} (k_{\perp}^2 + k_{||}^2) \Phi(k) e^{-ik_{\perp}\chi_{\perp}} \int_0^{\chi_s} e^{-ik_{||}\chi'} \chi' \left(1 - \frac{\chi'}{\chi_s}\right) d\chi'. \quad (\text{A24})$$

Now we can calculate the relative perturbed angular distance to the background angular distance as follows

$$\frac{\delta D}{D_0} = - \int_0^{\chi_s} \int \frac{d^3 k}{(2\pi)^3} (k_\perp^2 + k_\parallel^2) \Phi(k) e^{-ik_\perp \chi_\perp} e^{-ik_\parallel \chi'} \chi' \left(1 - \frac{\chi'}{\chi_s}\right) d\chi'. \quad (\text{A25})$$

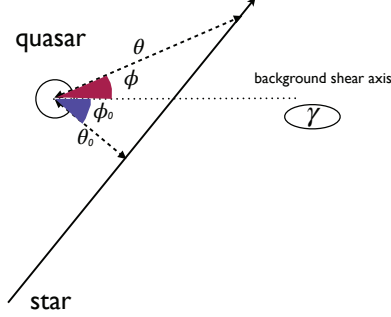


FIG. 8: Schematics of stellar microlensing in background shear field.

In this integral, the longitudinal modes with wave length smaller than  $\chi_s$  can cancel the effect of each other and only  $k_\parallel < \chi_s^{-1}$  modes have non-zero contribution in the integration. On the other hand in order to have short transient events the width of modes must be much smaller than the longitudinal size,  $k_\parallel \ll k_\perp$ . Since the flux of source at the position of observer is proportional to the inverse of square of angular distance,  $F \propto D^{-2}$ , the magnification in terms of angular distance can be written as:

$$A = \frac{F}{F_0} = \left(1 + \frac{D_1}{D_0}\right)^{-2}. \quad (\text{A26})$$

So perturbation in the magnification obtain as

$$\delta A = 2 \int_0^{\chi_s} \int \frac{d^3 k}{(2\pi)^3} k_\perp^2 \Phi(k) e^{-ik_\perp \chi_\perp} e^{-ik_\parallel \chi'} \left(1 - \frac{\chi'}{\chi_s}\right) \chi' d\chi', \quad (\text{A27})$$

This expression is identical to what is obtained from the geodesics method in equation (14). We note that  $\delta A$  is a time dependent function as the transverse position of the structures changes with respect to our line of sight.

## Appendix B: Temporal power spectrum of microlensing

In this appendix, we compute the expected contribution to the magnification temporal power spectrum due to stellar microlensing events. We first note that the magnification  $A$  is given by:

$$A^{-1} = A_0^{-1} + 2\gamma(\theta_E/\theta)^2 \cos(2\phi) - (\theta_E/\theta)^4, \quad (\text{B1})$$

where  $A_0$  and  $\gamma$  are magnification and shear of the smooth background.  $\phi$  is the angle between the principal axis of the background shear field, and the line that connects star to the quasar in the sky. For a star moving on a straight line, with impact parameter  $\theta_0$  (see Fig. 8) and proper motion  $\dot{\theta}$ , the Fourier transform of Eq. (B1) is:

$$A_0^{-2} \delta A_\omega \simeq \frac{\pi \theta_E^2}{\dot{\theta} \theta_0} e^{-i\omega t_0 - |\omega \theta_0 / \dot{\theta}|} \left[ \frac{\theta_E^2}{2\theta_0^2} (1 + |\omega \theta_0 / \dot{\theta}|) + 2\gamma |\omega \theta_0 / \dot{\theta}| e^{2i\phi_0 \cdot \text{sgn}(\omega)} \right], \quad (\text{B2})$$

where  $t_0$  and  $\phi_0$  are time and  $\phi$  when  $\theta = \theta_0$ . To find the total temporal power spectrum of magnification, we have to add the  $\delta A_\omega$ 's from all the stars. However, assuming a random distribution of stars, the contributions only add in quadratures:

$$P_{\text{stars}}(\omega) = A_0^4 T_{\text{obs}}^{-1} \sum_{\text{stars}} \frac{\pi^2 \theta_E^4}{\dot{\theta}^2 \theta_0^2} e^{-2|\omega \theta_0 / \dot{\theta}|} \left| \frac{\theta_E^2}{2\theta_0^2} (1 + |\omega \theta_0 / \dot{\theta}|) + 2\gamma |\omega \theta_0 / \dot{\theta}| e^{2i\phi_0} \right|^2, \quad (\text{B3})$$

or

$$\begin{aligned}
\sigma_{\text{stars}}^2 &\equiv \int_{T_{\text{obs}}^{-1}}^{\infty} P_{\text{stars}}(\omega) \frac{d\omega}{2\pi} \\
&= \sum_{\text{stars}} \frac{\pi A_0^4 \theta_E^4}{32 \theta_0^7 \dot{\theta}^3 T_{\text{obs}}^3} \exp\left(-\frac{2\theta_0}{\dot{\theta} T_{\text{obs}}}\right) \left[ 2(\theta_0^2 \theta_E^4 + 16\gamma^2 \theta_0^6) + 2\theta_0(3\theta_E^4 + 16\gamma^2 \theta_0^4) \dot{\theta} T_{\text{obs}} + (5\theta_E^4 + 16\gamma^2 \theta_0^4) \dot{\theta}^2 T_{\text{obs}}^2 \right]
\end{aligned} \tag{B4}$$

where we have suppressed the dependence of the parameters  $\theta_E, \theta_0, \phi_0$  and  $\dot{\theta}$  on the star, and further used  $\langle e^{i\phi_0} \rangle = 0$  in the last equality.

Therefore, we see that typical events with  $t(\theta) \sim \frac{\theta_0}{\dot{\theta}} \sim 10^2$  yr's (Eq. 38), are suppressed by exponential of

---

$t(\theta)/T_{\text{obs}} \sim 10^2$  over relevant time-scales of  $T_{\text{obs}} \sim \text{yr}$ , and thus are completely negligible.